Acetylene and Ethylene Complexes of Copper and Silver Atoms. Matrix Isolation ESR Study

Paul H. Kasai,* D. McLeod, Jr., and T. Watanabe†

Contribution from the Union Carbide Corporation, Tarrytown Technical Center, Tarrytown, New York 10591. *Received June 6, 1979*

Abstract: Acetylene and ethylene complexes of Cu and Ag atoms were generated in rare-gas matrices and were examined by electron spin resonance spectroscopy. The study revealed that Cu atoms form both mono- and diligand complexes, $Cu(C_2H_2)_{n=1,2}$ and $Cu(C_2H_4)_{n=1,2}$, while Ag atoms form a bona fide complex with a diethylene group only, hence $Ag(C_2H_4)_2$. The g tensors and the hyperfine coupling tensors to the metal and hydrogen nuclei were determined and analyzed. It is shown that all these complexes have π-coordinated structures consistent with the Dewar-Chatt-Duncanson scheme. The semifilled orbital of the monoligand complexes is an s-p hybridized orbital of the metal atom pointing away from the ligand moiety. The diligand complexes have D_{2h} symmetry; the metal atom is flanked by two ligand molecules oriented parallel to each other. The semifilled orbital of the latter is essentially the p orbital of the metal atom parallel to the ligand molecules. In the case of Ag and acetylene, when allowed to react in the vapor phase, an Ag-acetylene adduct having the vinyl structure was generated.

Introduction

Metal-atom chemistry in which vaporized metal atoms are trapped and allowed to react with organic and inorganic molecules condensed at cryogenic temperature has been the subject of many recent investigations.[1] Reactions between transition-metal atoms and small unsaturated organic molecules such as acetylene or ethylene are of particular interest because of their relevance to organometallic syntheses and transition-metal catalysis.

Recently we communicated on electron spin resonance (ESR) detections of Ag atom–ethylene and Cu atom–acetylene complexes generated in rare-gas matrices by cocondensation of the respective metal atoms and the organic ligand molecules.[2,3] Concurrently, Ozin and his co-workers also succeeded in generating ethylene complexes of Cu, Ag, and Au atoms in rare gas matrices, and observed and assigned the electronic (UV, visible) and vibrational (IR, Raman) spectra of $Cu(C_2H_4)_{n=1,2,3}$,[4] $Ag(C_2H_4)$,[5] and $Au(C_2H_4)$.[6]

The purpose of the present report is to describe and analyze in detail the ESR spectra of Ag–ethylene and Cu–acetylene complexes communicated earlier and those of Ag–acetylene and Cu–ethylene complexes observed thenceforth.

Numerous olefin molecules are known to complex with univalent Cu or Ag cations.[7] As originally suggested by Dewar,[8] Chatt, and Duncanson,[9] the formation of these complexes is attributed to two dative bonds, one of "donation" by the filled π orbital of the olefin to the vacant s orbital of the cation (located equidistant from the two unsaturated carbon atoms), and the other of "back-donation" by the filled d orbital of the cation into the vacant antibonding π orbital. The present series of ESR experiments revealed that, while Cu atoms form mono- and diligand complexes of both acetylene and ethylene, Ag atoms form a bona fide complex only with a diethylene group. The spectrum previously assigned to $Ag(C_2H_4)$ in ref 2 has been reassigned to $Ag(C_2H_4)_2$. It is concluded that all of these complexes have π-coordinated structures consistent with the dative bonds of the Dewar–Chatt–Duncanson scheme. Molecular orbital consideration suggests, however, that the dative bond of "back-donation" is much more significant than the other in these complexes. In the special case of Ag and acetylene, when allowed to react in the vapor phase, an Ag–acetylene adduct having the vinyl form was generated.

* To whom correspondence should be addressed at: IBM (78V-906), Box 390, Poughkeepsie, N.Y. 12602.

† Department of Chemistry, University of Tokyo, Tokyo, Japan.

Experimental Section

The experimental setup designed to trap high-temperature vapor-phase species in a rare-gas matrix at liquid helium temperature and to observe the ESR spectra of the resulting matrix was described earlier.[10] In the present series of experiments, Cu and Ag atoms were vaporized from tantalum cells resistively heated to ~1350 and ~1450 °C, respectively, and were trapped in rare-gas (Ar or Ne) matrices containing acetylene or ethylene. The concentrations of acetylene and ethylene were varied usually from 0.3 to 10 mol % and those of the metal atoms were maintained at ~0.1 mol %. The spectometer frequency locked to the sample cavity was 9.425 GHz and all the spectra were observed while the matrices were maintained at ~4 K.

Deuterated acetylene (C_2D_2) and ethylene (C_2D_4) (enrichment >99%) were obtained from Merck and Co., Inc.

Spectra and Assignments

Cu Atom–Acetylene Complexes. The ESR spectrum observed from an argon matrix containing Cu and C_2H_2 (2%) is shown in Figure 1. Three different types of signals (A, B, and C) are recognized as indicated. The signals A are due to isolated Cu atoms ($3d^{10}4s^1$). Owing to the large hyperfine interaction with ^{63}Cu (natural abundance = 69%, $I = 3/2$, $\mu = 2.2206\beta_N$) and ^{65}Cu (natural abundance = 31%, $I = 3/2$, $\mu = 2.3790\beta_N$) only two transitions of Cu atoms are observable: one transition corresponding to the "NMR" transition $M_S = -1/2$, $M_I = -1/2 \rightarrow -3/2$ occurs at 1.5 and 2.0 kG for ^{63}Cu and ^{65}Cu, respectively, and the other corresponding to the ESR transition $M_S = -1/2 \rightarrow +1/2$, $M_I = -3/2$ occurs at 5.8 and 6.0 kG.[11] The signals B and C were observed only when the matrices contained both Cu and acetylene. As indicated in the figure, the signals B were recognized as two sets of quartets arising from the hyperfine interactions with ^{63}Cu and ^{65}Cu, respectively. The spectrum C consists of many hyperfine components placed symmetrically within a narrow range (±200 G) of the position corresponding to $g = 2.00$. It is shown in Figure 2a in an expanded scale.

When the matrix was prepared using less acetylene (0.3 mol %), the Cu atom signals A became stronger, the B signals appeared essentially unchanged, while the C signals became barely observable. When the acetylene concentration was increased to 10 mol %, the C signals became extremely intense, but the A and B signals were no longer observed. It is thus strongly suggested that a greater number of acetylene molecules are involved in complex C than in B. Figure 2b shows the spectrum C observed when the matrix was prepared using perdeuterioacetylene (C_2D_2, 2 mol %). No discernible effect of the isotopic substitution was noted for the B signals. The quartet pattern resolved in Figure 2b is also attributed to the

0002-7863/80/1502-0179$01.00/0

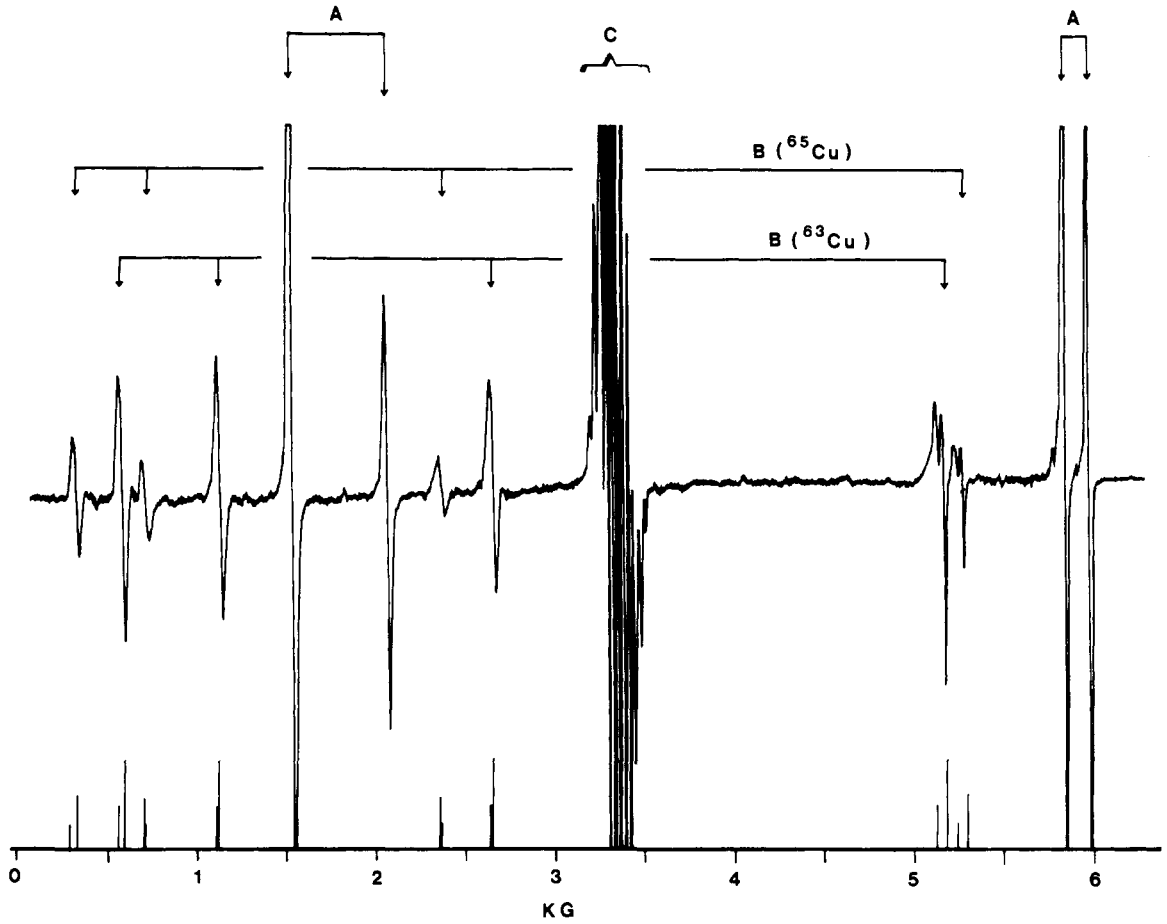

Figure 1. ESR spectrum of an argon matrix containing Cu and acetylene (2 mol %). The bars indicate the computed resonance positions of the B signals based upon the parameters given in the text.

Table I. Observed Resonance Positions of the $Cu(C_2H_2)$ and $Cu(C_2H_4)$ Complexes Generated in Argon Matrices (Given in G; the Accuracy ±2 G; the Microwave Frequency = 9425 MHz)

complex	hyperfine component (M_I)			
	$+3/2$	$+1/2$	$-1/2$	$-3/2$
$^{63}Cu(C_2H_2)$	563 (∥)	1138	2668	5148 (∥)
	598 (⊥)			5197 (⊥)
$^{65}Cu(C_2H_2)$	306 (∥)	724	2376	5254 (∥)
	341 (⊥)			5300 (⊥)
$^{63}Cu(C_2H_4)$	622 (∥)	1227	2733	5118 (∥)
	666 (⊥)			5181 (⊥)
$^{65}Cu(C_2H_4)$	369 (∥)	852	2478	5223 (∥)
	415 (⊥)			5287 (⊥)

hyperfine structure due to the Cu nuclei; the difference between the coupling tensors of ^{63}Cu and ^{65}Cu is too small to be resolved and the broader line width of the outer components is attributed to the anisotropy of the coupling tensors. A careful examination of Figures 2a and 2b shows that the spectral pattern of Figure 2a is an overlapping quartet of quintets, the quartet spacing being equal to that seen in Figure 2b and the quintet feature being that expected from the hyperfine interaction with four *equivalent* protons. It is proposed, therefore, that the spectrum B be assigned to the monoacetylene complex $Cu(C_2H_2)$ and the spectrum C to the diacetylene complex $Cu(C_2H_2)_2$.

Figure 3 shows the highest and the lowest field components ($M_I = \pm 3/2$) of the B signals recorded in an expanded scale. The line shape of the components is that expected from an ensemble of randomly oriented radicals having uniaxially asymmetric g and/or hyperfine coupling tensors. The remaining components ($M_I = \pm 1/2$) of the B signals, however, appeared isotropic with the peak-to-peak line width of ~30 G. The observed resonance positions of the B signals are given in Table I. Clearly the spacings of these signals are such that the usual second-order solution of a spin Hamiltonian cannot be applied for their analysis.

Asserting that the principal axes of the g tensor and the hyperfine coupling tensor coincide, and that the z axis lies parallel to the external field, a spin Hamiltonian of a radical with $S = 1/2$ and one magnetic nucleus can be written and rearranged as follows:

$$\mathcal{H}_{spin} = g_z\beta HS_z + AS_zI_z + BS_xI_x + CS_yI_y$$
$$= g_z\beta HS_z + AS_zI_z + \left(\frac{B+C}{4}\right)(I_+S_- + I_-S_+)$$
$$+ \left(\frac{B-C}{4}\right)(I_+S_+ + I_-S_-) \quad (1)$$

where A, B, and C are the elements of the principal hyperfine coupling tensor. If the anisotropy of the coupling tensor is small, $(B - C)/2 \ll (B + C)/2 \simeq A$, as it is in the present case, the last term in the above expression may be neglected. We thus have

$$\mathcal{H}_{spin} = g_z\beta HS_z + AS_zI_z + \left(\frac{B+C}{4}\right)(I_+S_- + I_-S_+) \quad (2)$$

The secular determinant derived from Hamiltonian (2) is tridiagonal and, thus, can be expanded exactly using a continued fraction technique.[12] From the eigenvalues expressed in the continued fraction form, the following "continued expression" can be obtained for the resonance field of each hy-

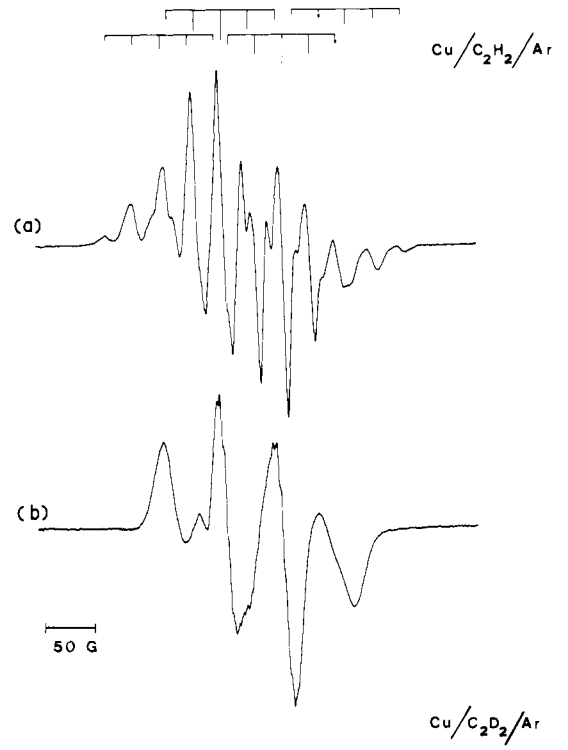

Figure 2. (a) The C signal (of Figure 1) shown in expanded scale. (b) The C signal observed when perdeuterioacetylene (2 mol %) was used.

perfine component given by $M_1 = M$.

$$H_z(M) = H_z^0 - MA' - F - G \qquad (3)$$

where

$$F = \frac{Q^2\,[I(I+1) - M(M+1)]}{H_z(M) + (M + \frac{1}{2})A + F}$$

$$G = \frac{Q^2[I(I+1) - M(M-1)]}{H_z(M) + (M - \frac{1}{2})A' + G}$$

and

$$H_z^0 = \frac{h\nu}{g_z\beta}$$

$$A' = \frac{A}{g_z\beta},\ B' = \frac{B}{g_x\beta},\ C' = \frac{C}{g_y\beta}$$

$$Q = \frac{1}{4g_z}(B'g_x + C'g_y)$$

The expressions for the resonance positions $H_x(M)$ and $H_y(M)$ can be readily generated by appropriate permutation of (g_x, g_y, g_z) and (A', B', C') in eq 3.

From the observed resonance positions of the $M_1 = \pm\frac{3}{2}$ components of $^{63}Cu(C_2H_2)$, where $H_\parallel(\pm\frac{3}{2}) = H_z(\pm\frac{3}{2})$ and $H_\perp(\pm\frac{3}{2}) = H_x(\pm\frac{3}{2}) = H_y(\pm\frac{3}{2})$, and the set of eq 3 developed above for $H_x(M)$, $H_y(M)$, and $H_z(M)$, the consistent set of g and hyperfine coupling constants can be determined readily through a computer-assisted iteration process. The g tensor and the hyperfine coupling tensor to the ^{63}Cu nucleus of $Cu(C_2H_2)$ were thus determined as follows:

$$g_\parallel = 2.015 \pm 0.002$$

$$g_\perp = 1.982 \pm 0.002$$

$$A_\parallel = 4.111 \pm 0.005\ \text{GHz}$$

$$A_\perp = 4.053 \pm 0.005\ \text{GHz}$$

The resonance positions of $^{63}Cu(C_2H_2)$ and $^{65}Cu(C_2H_2)$ computed from eq 3 based upon these tensors and the known

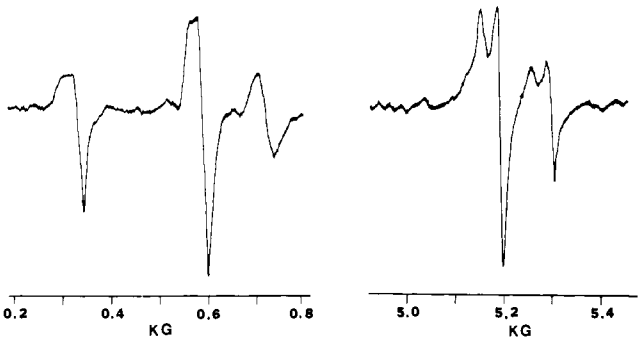

Figure 3. The highest and the lowest field components ($M_1 = \pm\frac{3}{2}$) of the B signals (of Figure 1) shown in expanded scale.

ratio of the nuclear magnetic moments of ^{63}Cu and ^{65}Cu are shown at the bottom of Figure 1; the shorter and longer bars indicate the parallel and perpendicular components, respectively.

The C signals of diacetylene complexes (Figures 2a and 2b) can be dealt with by the usual second-order solution of a spin Hamiltonian. Resorting to the method of computer simulation (of the ESR spectrum of randomly oriented radicals),[13] the following g and hyperfine coupling tensors were determined for $Cu(C_2H_2)_2$.

$$g_\parallel = 1.997 \pm 0.002$$

$$g_\perp = 1.997 \pm 0.002$$

$$A_\parallel(^{63}Cu) \simeq 0\ \text{G}$$

$$|A_\perp(^{63}Cu)| = 68 \pm 5\ \text{G}\ (190 \pm 14\ \text{MHz})$$

$$A_\parallel(H) = A_\perp(H) = 28 \pm 3\ \text{G}$$

The computer-simulated spectra of $Cu(C_2H_2)_2$ and $Cu(C_2D_2)_2$ based upon these parameters are compared with the observed spectra in Figure 4. The signal D indicated by an arrow in Figure 4c is believed to be caused by an impurity in the C_2D_2 source. Though its intensity increased with increasing C_2D_2 concentration, no signal corresponding to it was observed in the spectra obtained using normal acetylene.

Cu Atom–Ethylene Complexes. The ESR spectrum of an argon matrix containing Cu and C_2H_4 (2%) is shown in Figure 5. In addition to the A signals due to isolated Cu atoms, two types of signals B and C were recognized and were assigned to the monoethylene complex $Cu(C_2H_4)$ and diethylene complex $Cu(C_2H_4)_2$, respectively. As in the case of Cu and acetylene, when the concentration of ethylene was decreased (~0.3 mol %), the Cu atom signals A became stronger, the B signals remained unchanged, and the C signals became weaker. When the ethylene concentration was increased to 10 mol %, only the C signals were observed.

The assignment of the B signals to the monoethylene complex is based upon the similarity of both the intensity characteristic and the overall spectral pattern to those of the Cu–monoacetylene complex discussed above. No discernible change was noted in these signals when the experiment was repeated using C_2D_4. The observed resonance positions of the B signals of the Cu–ethylene system are also given in Table I. Using eq 3 and the observed resonance positions of the $M_1 = \pm\frac{3}{2}$ components of $^{63}Cu(C_2H_4)$, the following g and hyperfine coupling tensors were determined.

$$g_\parallel = 2.018 \pm 0.005$$

$$g_\perp = 1.976 \pm 0.005$$

$$A_\parallel = 4.045 \pm 0.010\ \text{GHz}$$

$$A_\perp = 3.974 \pm 0.010\ \text{GHz}$$

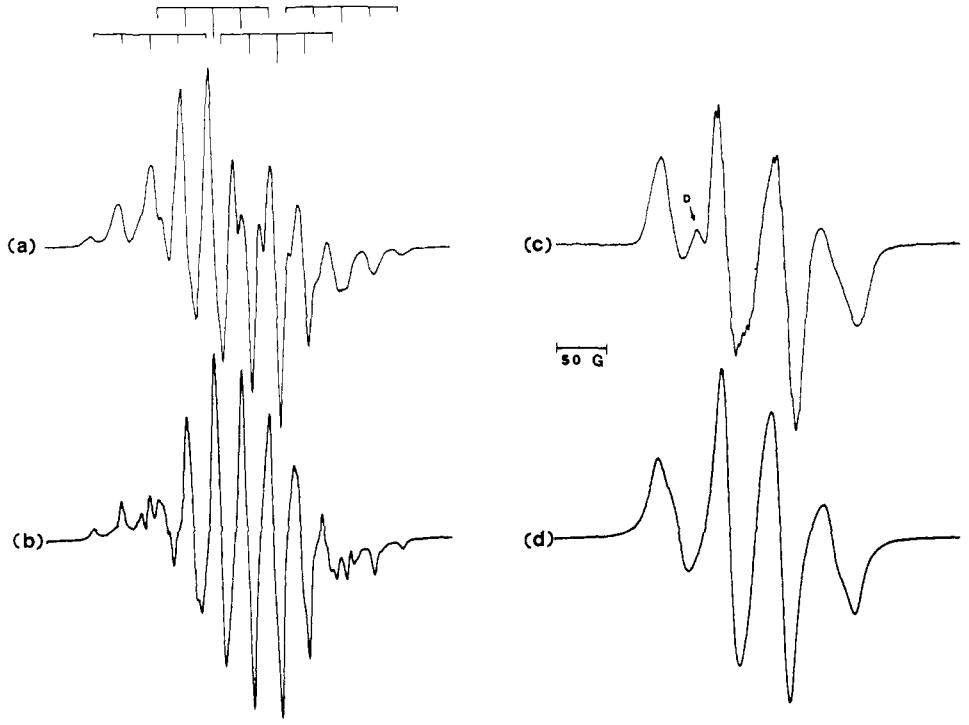

Figure 4. (a) Observed and (b) simulated spectra of $Cu(C_2H_2)_2$. (c) Observed and (d) simulated spectra of $Cu(C_2D_2)_2$.

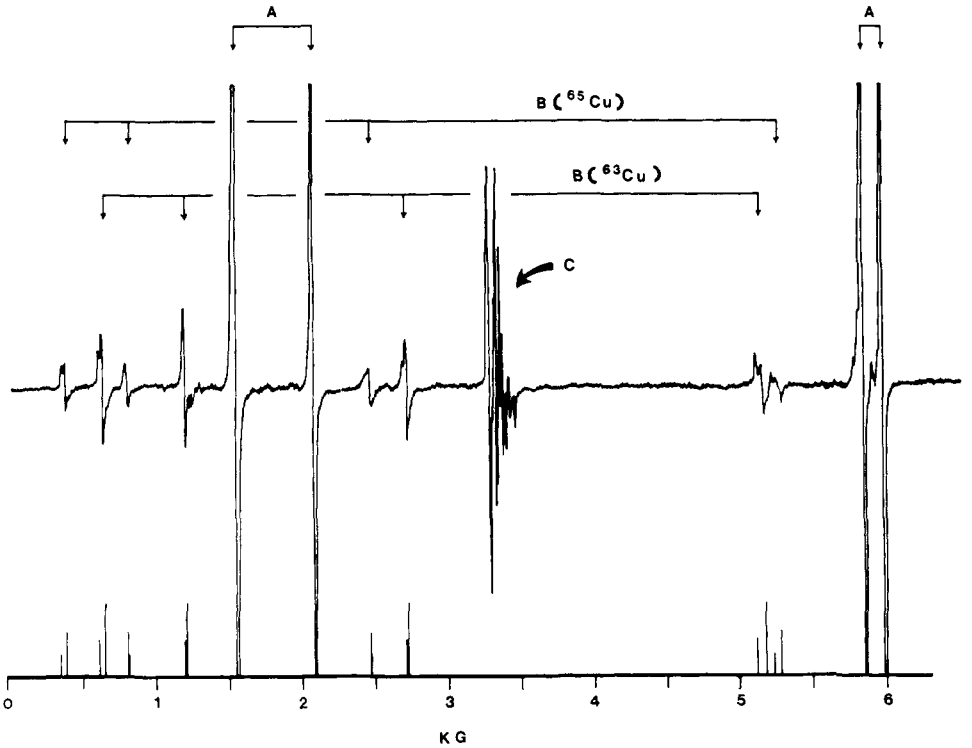

Figure 5. ESR spectrum of an argon matrix containing Cu and ethylene (2 mol %). The bars indicate the computed resonance positions of the B signals based upon the parameters given in the text.

The resonance positions of $^{63}Cu(C_2H_4)$ and $^{65}Cu(C_2H_4)$ computed from eq 3 based upon these tensors and the known ratio of the nuclear magnetic moments of ^{63}Cu and ^{65}Cu are shown at the bottom of Figure 5.

Figure 6 shows, in an expanded scale, the C spectra of the Cu-ethylene system obtained when normal ethylene (C_2H_4, 2 mol %) and perdeuterioethylene (C_2D_4, 2 mol %) were used, respectively. Unlike the case of Cu and acetylene, the C spectrum of the Cu-ethylene system showed no resolved hyperfine structure due to protons, though the deuteration effected a small but distinct decrease of the line width. The assignment of the C signals to the Cu-diethylene complex is thus somewhat conjectural. It is based on (1) the dependency of the intensity upon the ethylene concentration, (2) the similarity of the Cu hyperfine coupling tensor to that of $Cu(C_2H_2)_2$ as will be shown later, and (3) the report by Ozin et al.,[4] who, based on an IR study, concluded that the major complexes formed in the Cu/C_2H_4 (1-10 mol %)/Ar system condensed at 10 K are $Cu(C_2H_4)$ and $Cu(C_2H_4)_2$.

The spectrum of $Cu(C_2D_4)_2$ (Figure 6b) is much more

complex than that of $Cu(C_2D_2)_2$ (Figure 2b); the increased complexity is in part due to increased anisotropy of both the g tensor and the hyperfine coupling tensor to the Cu nucleus. Figures 7a and 7b show respectively the observed spectrum of $Cu(C_2D_4)_2$ and its analysis based on an orthorhombic g tensor and an orthorhombic hyperfine coupling tensor to a nucleus of spin $3/2$. Figure 7c is the computer-simulated spectrum based on these tensors and the resonance positions derived from the usual second-order solution of a spin Hamiltonian. The simulated spectrum is in reasonable, but not in exact, agreement with the observed spectrum. The notable variances are the doublet pattern and the sharp upward signal indicated by arrows in Figure 7a. These anomalous features are attributed to the forbidden transitions ($\Delta M_s = \pm 1$, $\Delta M_I = \pm 1$ and ± 2) induced by the quadrupole interaction of the Cu nucleus.

For the radical with $S = 1/2$ and one magnetic nucleus with $I > 1/2$, a spin Hamiltonian including the nuclear quadrupole interaction may be written as follows:

$$\mathcal{H}_{spin} = g_x\beta H_x S_x + g_y H_y S_y + g_z\beta H_z S_z + A_x S_x I_x + A_y S_y I_y + A_z S_z I_z + P_x I_x^2 + P_y I_y^2 + P_z I_z^2 \quad (4)$$

where (g_x, g_y, g_z), (A_x, A_y, A_z), and (P_x, P_y, P_z) are the diagonal elements of the principal g tensor, the hyperfine coupling tensor, and the quadrupole tensor, respectively. A treatment of this Hamiltonian by second-order perturbation theory for an axially symmetric case ($g_x = g_y$, $A_x = A_y$, and $P_x = P_y$) has been shown by Bleaney.[14] The equations relating to the resonance positions of the normal and forbidden transitions, and the transition probabilities of the latter relative to the normal transitions, were reported. We have carried out a similar treatment of the Hamiltonian for an orthorhombic case and obtained the following equation of the resonance field for the transition $|M_s = 1/2, M_I = M\rangle \leftrightarrow |M_s = -1/2, M_I = M'\rangle$.

$$H_{M\to M'} = H_0 - \tfrac{1}{2}A(M + M') - \frac{A'}{8H_0}[2I(I+1) - M^2 - M'^2] + \frac{A''}{4H_0}(M - M') - \frac{A'''}{4H_0}(M^2 + M'^2) - \frac{3}{2}P(M^2 - M'^2) - \frac{1}{4A}[P'(2I^2 + 2I - 1) - 4P''(4I^2 + 4I - 1)](M + M') + \frac{1}{2A}(P' - 16P'')(M^3 + M'^3) \quad (5)$$

where $H_0 = h\nu/g\beta$

$$g^2 = g_z^2\cos^2\theta + (g_x^2\cos^2\phi + g_y^2\sin^2\phi)\sin^2\theta$$

and when the principal axes of the g, A, and P tensors are coincident

$$g^2A^2 = g_z^2A_z^2\cos^2\theta + (g_x^2A_x^2\cos^2\phi + g_y^2A_y^2\sin^2\phi)\sin^2\theta$$

$$A' = A_x^2(1 - U_x^2) + A_y^2(1 - U_y^2) + A_z^2(1 - U_z^2)$$

$$A'' = A_xA_yA_z/A$$

$$A''' = A_x^2U_x^2 + A_y^2U_y^2 + A_z^2U_z^2 - A^2$$

$$P = P_xU_x^2 + P_yU_y^2 + P_zU_z^2$$

$$P' = P_x^2 + P_y^2 + P_z^2 + P^2 - 2(P_x^2 + P_yP_z)U_x^2 - 2(P_y^2 + P_zP_x)U_y^2 - 2(P_z^2 + P_xP_y)U_z^2$$

$$P'' = P_x^2U_x^2 + P_y^2U_y^2 + P_z^2U_z^2 - P^2$$

Here θ and ϕ represent, in the usual manner, the direction of the magnetic field relative to the g tensor, and U_x, U_y, and U_z

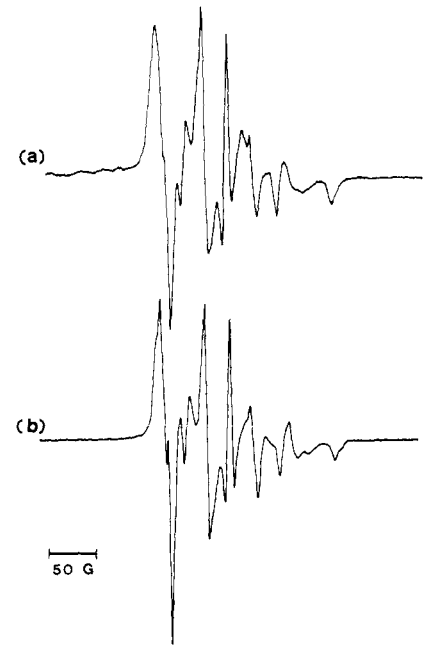

Figure 6. (a) The C signal (of Figure 5) shown in expanded scale. (b) the C signal observed when perdeuterioethylene (2 mol %) was used.

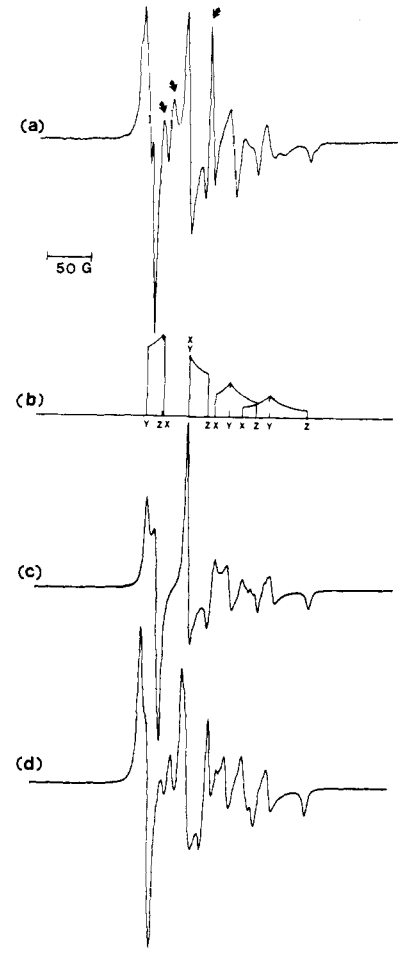

Figure 7. (a) The observed ESR spectrum of $Cu(C_2D_4)_2$. (b) The analysis of the spectrum based upon an orthorhombic g tensor and a hyperfine coupling tensor to a nucleus of $I = 3/2$. (c) The simulated spectrum based upon the assignment given above allowing only the normal transitions ($\Delta M_s = \pm 1$, $\Delta M_I = 0$). (d) The simulated spectrum based upon the same assignment allowing both the normal and forbidden transitions ($\Delta M_s = \pm 1$, $\Delta M_I = \pm 1$, ± 2) induced by the quadrupole interaction of the Cu nucleus.

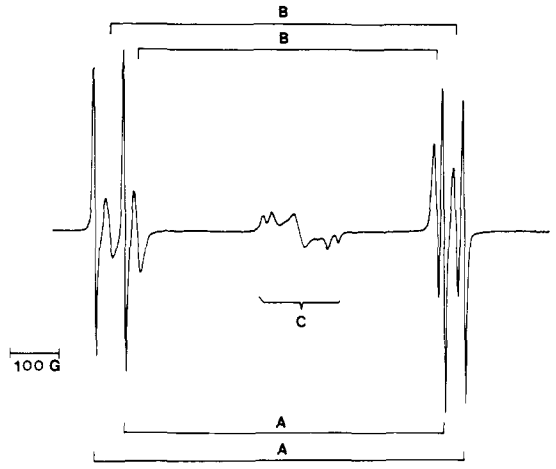

Figure 8. ESR spectrum of an argon matrix containing Ag and ethylene. Two sharp doublets (A) are due to Ag atoms. Two broad doublets (B) and the central signals (C) result from cocodensation of Ag and ethylene.

are the direction cosines of the axis of the nuclear quantization and are given by

$$U_x = \left(\frac{g_x A_x}{gA}\right) \cos\phi \sin\theta$$

$$U_y = \left(\frac{g_y A_y}{gA}\right) \sin\phi \sin\theta$$

$$U_z = \left(\frac{g_z A_z}{gA}\right) \cos\theta$$

The transition probabilities $\xi_{\Delta M}$ for the normal ($M' = M$) and forbidden transitions ($M' = M \pm 1, M \pm 2$) are given by

$$\xi_0 = 1 - \xi_{+1} - \xi_{-1} - \xi_{+2} - \xi_{-2}$$

$$\xi_{\pm 1} = \frac{4P''}{A^2}(2M \pm 1)^2[I(I+1) - M(M \pm 1)]$$

$$\xi_{\pm 2} = \frac{P'}{4A^2}[I(I+1) - M(M \pm 1)][I(I+1) - (M \pm 1)(M \pm 2)] \quad (6)$$

The powder-pattern spectrum simulation program was then modified to include these effects of the nuclear quadrupole interaction.

Figure 7d is the spectrum of $Cu(C_2D_4)_2$ simulated based upon the g and A tensors assessed previously (Figure 7b) and a quadrupole interaction tensor of the magnitude $|P| \simeq 0.1 \cdot |A|$ determined through a trial-and-error process. The diagonal elements of all the tensors used for the simulation follow.

tensor	x	y	z
g	2.010	2.005	1.989
$\|A\|$	30.0 G	47.0 G	56.0 G
P	5.2 G	−2.6 G	−2.6 G

Although the agreement is far from being perfect, the computed spectrum clearly supports the contention that the anomalous features cited earlier are attributes of a nuclear quadrupole interaction. Further attempts to refine the assignments were negated by the limitation of the second-order approximation used in deriving eq 5 and 6.

Ag Atom–Ethylene Complexes. The ESR spectrum of Ag atoms ($4d^{10}5s^1$) isolated in rare-gas matrices is known.[11] The spectrum consists of two sets of sharp doublets with the respective spacings of ~650 and ~750 G and of nearly equal intensity. The pattern is readily accounted for by the hyperfine interaction with the ^{107}Ag (natural abundance = 51%, $I = 1/2$, and $\mu = -0.1130\beta_N$) and ^{109}Ag (natural abundance = 49%, $I = 1/2$, and $\mu = -0.1299\beta_N$) nuclei. Figure 8 shows the ESR spectrum of an argon matrix containing Ag and C_2H_4 (3%). Three types of signals (A, B, and C) are indicated. The signals A are due to isolated Ag atoms, and the additional signals B and C result from the cocondensation of Ag and ethylene. Because of the extreme proximity of the signals A and B, the signals B were initially believed to be those of Ag atoms perturbed by "matrix site effects", and the signals C were assigned to the Ag–monoethylene complex.[2] However, we have since found that the relative intensities of the signals A, B, and C vary with the ethylene concentration with exactly the same dependency observed for the signals of the isolated metal atoms and the mono- and diligand complexes in the $Cu/C_2H_2/Ar$ and $Cu/C_2H_4/Ar$ systems. The effect was observed most conspicuously in the A, B, and C signals of the $Ag/C_2H_4/Ne$ system (Figure 9). Consequently, we now believe that the B and C signals of the $Ag/C_2H_4/Ar$ (or Ne) system should also be assigned to Ag atoms complexed with one and two ethylene molecules, respectively.

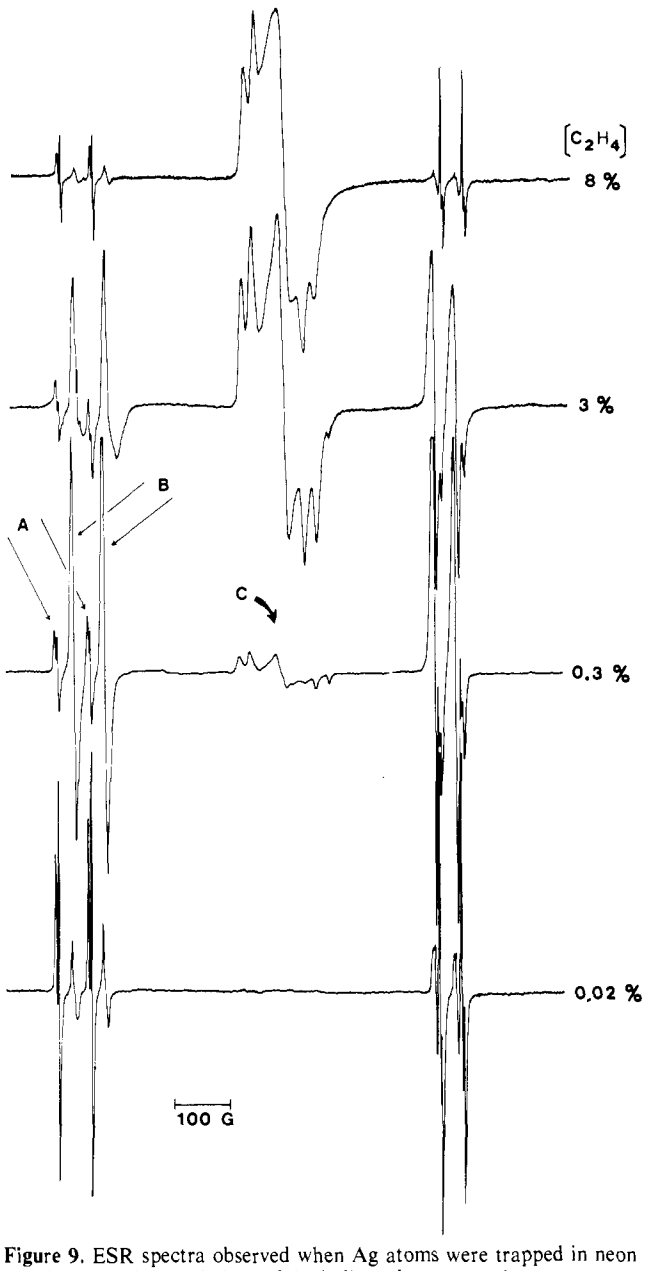

Figure 9. ESR spectra observed when Ag atoms were trapped in neon matrices containing ethylene of the indicated concentration.

The interaction leading to the association of Ag and one ethylene molecule must be weak, however; the coupling con-

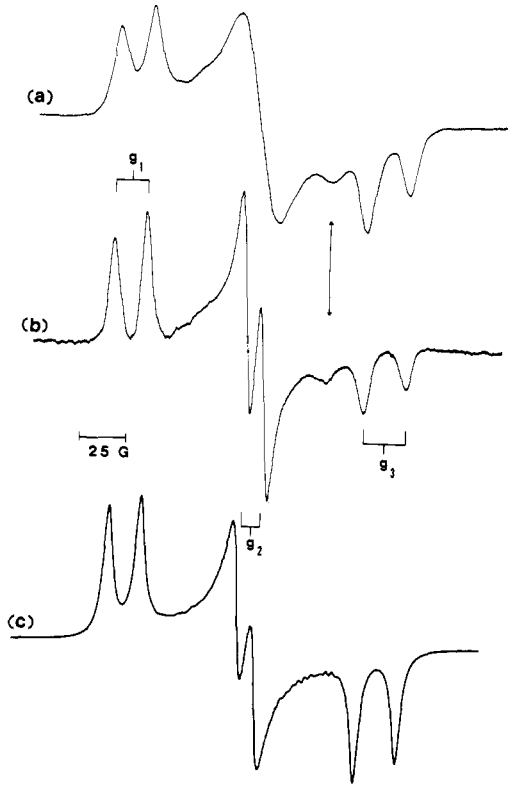

Figure 10. (a) ESR spectrum of $Ag(C_2H_4)_2$ generated in an argon matrix. (b) ESR spectrum of $Ag(C_2D_4)_2$ generated in an argon matrix. (c) Simulated spectrum of $Ag(C_2D_4)_2$ based upon the parameters given in the text.

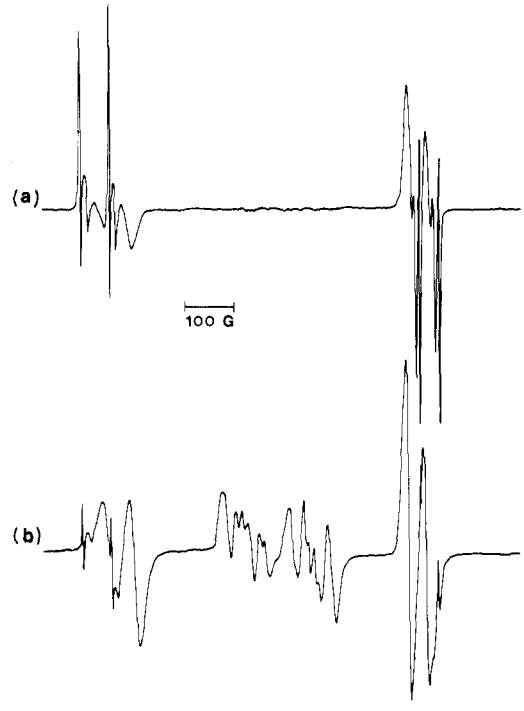

Figure 11. (a) ESR spectrum of an argon matrix containing Ag and C_2H_2 (7%). (b) ESR spectrum of an argon matrix prepared by trapping Ag and C_2H_2 introduced separately from the vapor sample inlet. The vapor-phase reaction is enhanced in this mode of preparation.

stant to the Ag nucleus in spectrum B is only 6% smaller than that of spectrum A. It has been shown that the coupling constant of Ag atoms isolated in rare-gas matrices varies as much as 5%, depending upon the particular gas used.[11] It thus seems inappropriate to consider the Ag-monoethylene entity encountered here as a bona fide complex. We will henceforth refer to this type of complex as pseudocomplex, and indicate it with the notation, e.g., Ag- - -C_2H_4.

The g value and the Ag coupling constant of Ag- - -C_2D_4 generated in the Ag/C_2D_4 (10%)/Ar system were determined as follows:

$$g = 1.998 \pm 0.001$$

$$A\ (^{107}Ag) = 1.659 \pm 0.001\ GHz$$

No discernible difference was noted between the spectra of the deuterated and nondeuterated species Ag- - -C_2D_4 and Ag- - -C_2H_4.

Figures 10a and 10b show, in an expanded scale, the C spectra of the Ag-diethylene complexes generated in the Ag/C_2H_4 (3%)/Ar and Ag/C_2D_4 (3%)/Ar systems, respectively. The deuteration clearly improves the resolution but does not alter the overall pattern. The spectral pattern must hence be attributed to the anisotropic g tensor of the complex and its hyperfine coupling tensor to the Ag nucleus. The spectrum of the deuterated species was hence assigned as indicated in the figure. Figure 10c shows the computer-simulated spectrum based upon this assignment and a Lorentzian line shape with the line width of 6 G. The coupling constant to the protons was then estimated as that which would give the best fit between the simulated and the observed spectrum of the nondeuterated complex assuming an isotropic interaction with eight equivalent protons. The parameters thus determined for $Ag(C_2H_4)_2$ are as follows:

$$g_1 = 2.042 \pm 0.001$$

$$g_2 = 2.002 \pm 0.001$$

$$g_3 = 1.961 \pm 0.001$$

$$|A_1(Ag)| = 16.8 \pm 0.5\ G$$

$$|A_2(Ag)| = 10.2 \pm 0.5\ G$$

$$|A_3(Ag)| = 22.2 \pm 0.5\ G$$

$$|A(H)| \cong 3 \pm 1\ G$$

The difference between the coupling tensors to the two Ag isotopes is too small to be resolved. The extra peak indicated by an arrow in the observed spectrum is probably due to Ag complexed with ethylene oligomers $(C_2H_4)_{n\geq 3}$. Its prominence increased with the increasing ethylene concentration of the matrix.

Ag Atom–Acetylene Complexes. When Ag atoms were trapped in argon matrices containing acetylene (0.1–20%), no ESR signals attributable to a bona fide complex were observed; only the signals due to isolated Ag atoms (the A signals) and those of pseudocomplexes (the B signals) were observed. See Figure 11a. A careful examination of the spectra revealed, however, three different types of B signals (B_1, B_2, and B_3). The A and B_1 signals dominated the spectra of matrices with low acetylene content (<3%), and the B_2 and B_3 signals dominated the spectra of matrices with medium (5–7%) and high (>10%) acetylene contents, respectively. Figure 12 shows, in an expanded scale, the lower field components of the A and B spectra observed from the representative Ar matrices. One may note that the matrix compositions conducive to the generation of the B_1 and B_2 species are very similar to those favoring the formation of $Cu(C_2H_2)$ and $Cu(C_2H_2)_2$, respectively, in the $Cu/C_2H_2/Ar$ system. We propose that the B_1, B_2, and B_3 spectra be assigned to Ag- - -C_2H_2, Ag- - -$(C_2H_2)_2$, and Ag- - -$(C_2H_2)_{n\geq 3}$. The assignment implies the formation

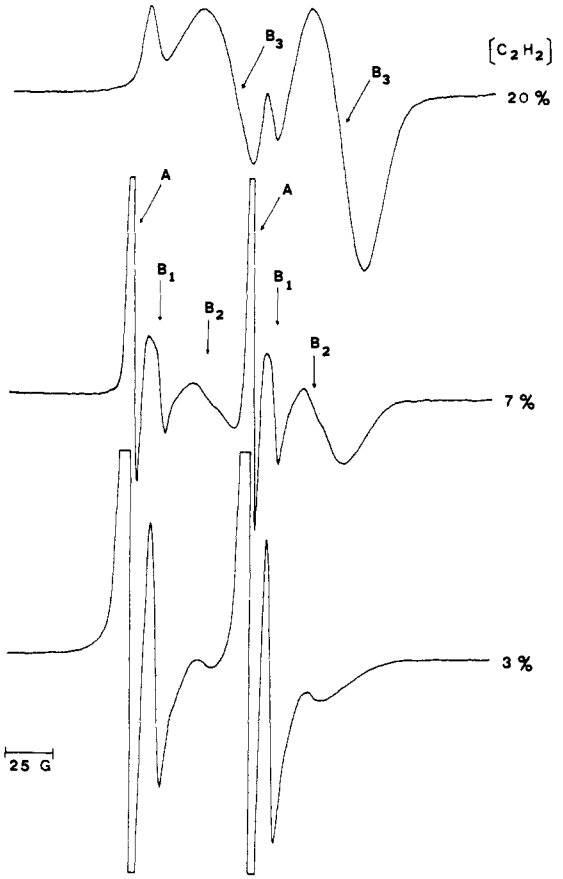

Figure 12. ESR spectra (the lower field components of the A and B doublets) observed when Ag atoms were trapped in argon matrices containing acetylene of the indicated concentration.

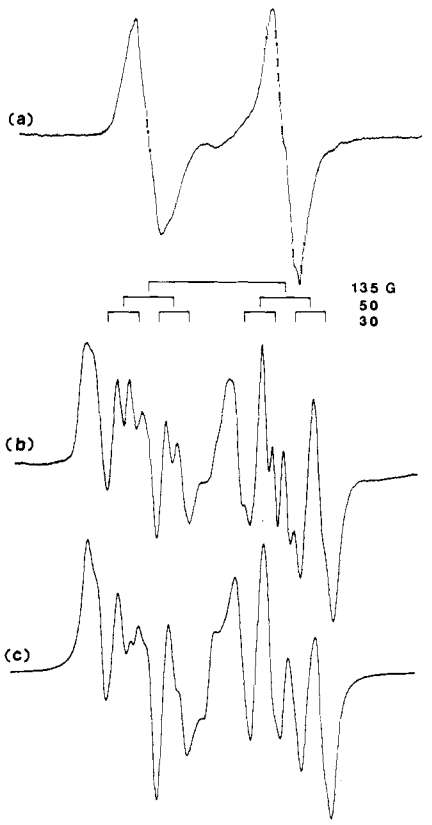

Figure 13. (a) ESR spectrum of Ag-C_2D_2 adduct trapped in an argon matrix. (b) ESR spectrum of Ag-C_2H_2 adduct trapped in an argon matrix. (c) Simulated spectrum of Ag-C_2H_2 based upon the parameters given in the text.

and the presence of acetylene dimers and oligomers in rare-gas matrices. The formation and the presence of dimers and oligomers of ethylene in argon matrices have been demonstrated recently in the IR work of Rytter and Gruen.[15]

The g values and the Ag coupling constants of the B_1, B_2, and B_3 pseudocomplexes generated in argon matrices were determined as follows.

	g	A (^{107}Ag), GHz
B_1	2.000 ± 0.001	1.753 ± 0.001
B_2	1.999 ± 0.001	1.657 ± 0.001
B_3	1.997 ± 0.001	1.611 ± 0.001

The coupling constants given above represent the lowering by 3, 8, and 11%, respectively, from the coupling constant of Ag atoms isolated in an argon matrix (1.809 GHz).[11] No discernible difference was noted between the spectra of the deuterated and nondeuterated Ag-acetylene pseudocomplexes. We conclude that, within rare-gas matrices maintained at liquid helium temperature, Ag atoms do not interact with acetylene to form a bona fide complex.

Figure 11b shows the ESR spectrum of an argon matrix which was prepared by trapping Ag atoms and acetylene introduced separately from Ar gas through the vapor phase sample inlet.[10] The cryostat geometry is such that, in this mode of operation, the Ag atoms traverse through the acetylene vapor prior to condensation. The spectrum consists of strong B_3 signals and new signals of comparable intensity in the central region. The latter must be attributed to radicals resulting from reactions in the vapor phase. The central signals observed from the matrices prepared by this "vapor phase reaction" mode using C_2D_2 and C_2H_2 are shown in Figures 13a and 13b.

The doublet pattern resolved in Figure 13a has a spacing of ~135 G. A careful examination of Figure 13b reveals that the spectrum is essentially a doublet of doublets of doublets with the respective spacings of 135, 50, and 30 G as indicated. The doublet structure of 135 G seen in both Figures 13a and 13b is thus attributed to the Ag nucleus, and those of 50 and 30 G seen in Figure 13b are attributed to the interactions with two nonequivalent protons. We propose to assign the spectrum to the Ag-acetylene adduct having the vinyl structure shown below and to ascribe the larger proton splitting to the β proton.

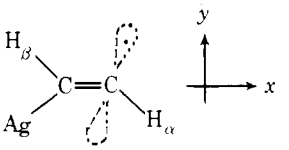

The unpaired electron is thus localized in the nonbonding, predominantly p_y orbital of the terminal carbon. The large, essentially isotropic hyperfine interactions with the Ag nucleus and the β proton are accounted for by the direct overlap of the p_y orbital with the valence orbitals of these nuclei.

A close inspection of the doublet in Figure 13a reveals, however, that the line widths of the two components are different, and are both larger than that expected from the corresponding coupling constants to the two deuterons. These features must arise from the anisotropies of the g tensor and the hyperfine coupling tensor to the Ag nucleus. Figure 13c is the computer-simulated spectrum based upon the following anisotropic g tensor, coupling tensor to the Ag nucleus, and isotropic coupling tensors to the two protons.

	x	y	z
g	1.9913	2.0023	2.0149
A (Ag)	123 ± 5 G	135 ± 5 G	123 ± 5 G
A (H_β)	50 ± 5 G	50 ± 5 G	50 ± 5 G
A (H_α)	30 ± 5 G	30 ± 5 G	30 ± 5 G

Table II. *g* Tensors, Hyperfine Coupling Tensors to the Metal Nuclei, and Structures of Cu and Ag Complexes Examined

complex	*g* tensor	coupling tensor to the metal nucleus	other parameter	structure
$^{63}Cu(C_2H_2)$	$g_\parallel = 2.015 \pm 0.002$ $g_\perp = 1.982 \pm 0.002$	$A_\parallel = 4111 \pm 5$ MHz $A_\perp = 4053 \pm 5$ MHz	$\lvert A(H)\rvert \leq 5$ G	
$^{63}Cu(C_2H_4)$	$g_\parallel = 2.018 \pm 0.005$ $g_\perp = 1.976 \pm 0.005$	$A_\parallel = 4045 \pm 10$ MHz $A_\perp = 3974 \pm 10$ MHz	$\lvert A(H)\rvert \leq 5$ G	
$Ag(C_2H_2)$	$g_1 = 2.015 \pm 0.002$ $g_2 = 2.002 \pm 0.002$ $g_3 = 1.991 \pm 0.002$	$A_1 = 123 \pm 5$ G $A_2 = 135 \pm 5$ G $A_3 = 123 \pm 5$ G	$A(H_\alpha) = 30$ G $A(H_\beta) = 50$ G	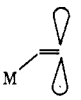
$Cu(C_2H_2)_2$	$g_\parallel = 1.997 \pm 0.002$ $g_\perp = 1.997 \pm 0.002$	$A_\parallel \simeq 0$ $A_\perp = 190 \pm 14$ MHz	$\lvert A(H)\rvert = 28$ G	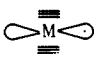
$Cu(C_2H_4)_2$	$g_1 = 2.010 \pm 0.002$ $g_2 = 2.005 \pm 0.002$ $g_3 = 1.989 \pm 0.002$	$A_1 = 84 \pm 6$ MHz $A_2 = 132 \pm 6$ MHz $A_3 = 156 \pm 6$ MHz	$\lvert A(H)\rvert \leq 3$ G quad coupl $P_1 = 5.2$ G $P_2 = P_3 = -2.6$ G	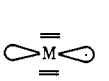
$Ag(C_2H_4)_2$	$g_1 = 2.042 \pm 0.001$ $g_2 = 2.002 \pm 0.001$ $g_3 = 1.961 \pm 0.001$	$A_1 = 16.8 \pm 0.5$ G $A_2 = 10.2 \pm 0.5$ G $A_3 = 22.02 \pm 0.5$ G	$\lvert A(H)\rvert \simeq 3$ G	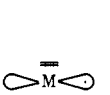

The overall agreement between the observed and the simulated spectra evidenced here is a strong substantiation to the proposed assignment. The coupling tensor to the α proton should have an anisotropy amounting to $\pm 10\rho$ G where ρ is the spin density at the p_y orbital of the terminal carbon.[13,16] Detailed features of the spectrum also depend upon the relative orientations of the *g* and the hyperfine coupling tensors. The discrepancies in detail between the observed and simulated spectra are due, most likely, to the neglect of these factors. The assessment of such factors from the observed spectrum is made difficult by the low symmetry of the adduct.

The presence of a barrier for the conversion of the pseudo-complex B_1 ($Ag\text{- - -}C_2H_2$) to the adduct of vinyl form is intriguing. It should also be reported that, in the present series of metal and ligand combinations, the matrix prepared by the "vapor phase reaction" mode yielded new radicals only in the case of Ag and acetylene.

Structures and Discussions

The *g* tensors, the hyperfine coupling tensors to the metal nuclei, and other spectroscopic parameters of the Cu and Ag bona fide complexes examined in the present study are compiled in Table II.

As stated earlier, the formation of molecular complexes between olefin molecules and univalent Cu and Ag cations is known. The two dative bonds suggested by Dewar[8] and Chatt and Duncanson[9] as being responsible for the formation of these complexes are depicted below.

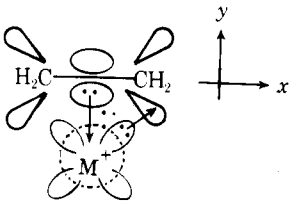

For a complex formed between an olefinic system and a neutral Cu or Ag atom, one may envisage one of the modes of interactions shown below. Scheme I represents the interaction of a charge-transfer complex. In II a metal–carbon σ bond is formed and the unpaired electron is localized at the terminal carbon. In schemes IIIA and IIIB the complex is formed by the dative bonds of the type proposed by Dewar[8] and Chatt and Duncanson,[9] and the two schemes differ in the disposition of

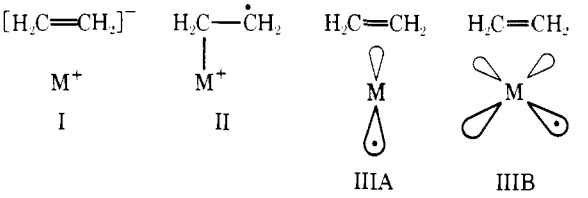

the unpaired electron. In the former scheme the unpaired electron is placed in a nonbonding s–p hybridized orbital pointing away from the double bond, and in the latter the unpaired electron is in a nonbonding d–p hybridized orbital pointing away from the double bond.

If the *g* tensor of a radical deviates little from that of a free electron, and the distribution of the unpaired electron in the vicinity of a magnetic nucleus is axially symmetric, the principal hyperfine coupling constants to the magnetic nucleus can be shown to be related to the isotropic term A_{iso} and the anisotropic, dipolar term A_{dip} as follows.[17]

$$A_\parallel = A_{iso} + 2A_{dip} \tag{7a}$$

$$A_\perp = A_{iso} - A_{dip} \tag{7b}$$

where

$$A_{iso} = g_e\beta_e g_n\beta_n \frac{8\pi}{3} |\Phi(0)|^2 \tag{8a}$$

$$A_{dip} = g_e\beta_e g_n\beta_n \left\langle \frac{3\cos^2\theta - 1}{2r^3} \right\rangle \tag{8b}$$

Here $|\Phi(0)|^2$ represents the spin density at the magnetic nucleus, r the separation between the unpaired electron and the magnetic nucleus, and θ the angle between r and the symmetry axis.

Let us examine how the spectroscopic parameters determined for $Cu(C_2H_2)$ and $Cu(C_2H_4)$ may elucidate their bonding schemes. The total absence of observable hyperfine structure due to protons immediately precludes the bonding schemes I and II. In each case the observed coupling tensor to the Cu nucleus is axially symmetric; the analysis of the tensor

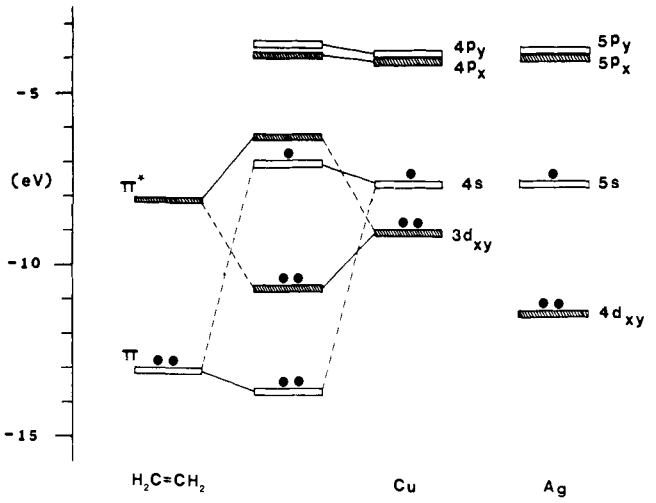

Figure 14. Schematic energy diagram showing the interaction of the π and π^* orbitals of ethylene with the valence orbitals of Cu leading to the formation of the π-coordinated complex. The corresponding orbital levels of Ag are also indicated.

in terms of eq 7 thus yields the following.

for $Cu(C_2H_2)$ $A_{iso}(^{63}Cu) = 4072 \pm 5$ MHz

$A_{dip}(^{63}Cu) = 19 \pm 2$ MHz

for $Cu(C_2H_4)$ $A_{iso}(^{63}Cu) = 3998 \pm 5$ MHz

$A_{dip}(^{63}Cu) = 24 \pm 3$ MHz

The semifilled orbitals of these complexes, if formed through scheme IIIB, would be given by $\Phi = a\phi(4p_x) - b\phi(3d_{xy})$ where $\phi(4p_x)$ and $\phi(3d_{xy})$ represent the respective atomic orbitals of Cu. The coupling tensor to the Cu nucleus would then consist of a small A_{iso} induced through core orbital polarization and a large A_{dip} attributable to the $3d_{xy}$ and/or $4p_x$ orbitals. The observed, large, essentially isotropic coupling constants to the Cu nuclei of these complexes rule out scheme IIIB.

We conclude that the complexes $Cu(C_2H_2)$ and $Cu(C_2H_4)$ are formed by the bonding scheme IIIA. The semifilled orbitals of these complexes are then given by

$$\Phi = a\phi(4s) - b\phi(4p_y) \quad (9)$$

Evaluation of A_{iso} and A_{dip} given in eq 8 in terms of this orbital yields

$$A_{iso} = a^2 g_e \beta_e g_n \beta_n \frac{8\pi}{3} |\phi(0)|^2_{4s}$$

$$A_{dip} = b^2 g_e \beta_e g_n \beta_n \frac{2}{5} \left\langle \frac{1}{r^3} \right\rangle_{4p}$$

Here $|\phi(0)|^2_{4s}$ and $\langle 1/r^3 \rangle_{4p}$ represent the indicated quantities of the Cu 4s and 4p atomic orbitals; the former may be assessed from the hyperfine coupling constant of the Cu atoms ($3d^{10}4s^1$) isolated in an argon matrix,[11] and the latter from the fine structure spacing of the atomic spectrum of Cu at $^2P(3d^{10}4p^1)$ state.[18] One then obtains $A_{iso} = 6151a^2$ (MHz) and $A_{dip} = 68b^2$ (MHz) and is led to the conclusion that the semifilled orbitals of these complexes consist of $\sim^2/_3$ of 4s and $\sim^1/_3$ of 4p orbitals of the Cu atom.

An intriguing question is why Cu and C_2H_4 monomer form a bona fide complex via scheme IIIA while Ag and C_2H_4 monomer form only a pseudocomplex. The EHT (extended Hückel theory) molecular orbital calculation places the bonding and antibonding π orbitals of ethylene at -13.2 and -8.2 eV, respectively. Figure 14 depicts schematically the π orbital levels of ethylene, the relevant valence orbitals of the Cu atom,[18] and their correlations to the pertinent levels of the Cu–ethylene complex. The exact energy levels of the complex are not known; they are drawn in the figure to indicate their positions relative to the interacting orbitals of Cu and C_2H_4. Inspection of the figure reveals immediately that the separation between Cu(4s) and the bonding π orbital of ethylene is too large to form an effective dative bond. The separation between Cu($3d_{xy}$) and the π^* orbital of ethylene, on the other hand, is small and an effective dative interaction is expected. The orbital resulting from the antibonding combination of the Cu($3d_{xy}$) and π^* orbitals would thus lie well above the orbital correlated to Cu(4s). Hence, taking cognizance of the repulsion imparted by the electrons of the bonding π orbital, the semifilled orbital of the $Cu(C_2H_4)$ complex is predicted to be essentially an s–p_y orbital of Cu pointing away from the double bond.

The energy levels of the relevant valence orbitals of the Ag atom[18] are also indicated in Figure 14. Here one notes that not only the separation between Ag(5s) and the bonding π orbital of ethylene but also the separation between Ag($4d_{xy}$) and the π^* orbital is too large to form an effective dative bond. Thus, the formation of a bona fide complex between Ag and C_2H_4 is not expected. The formation of the pseudocomplex Ag- - - C_2H_4 is attributed to the van der Waals type interaction prevailing in the low-temperature matrix environment.

The basic argument presented above should not alter when the ethylene moiety of the complex is replaced by acetylene. Therefore, while Cu and acetylene form a bona fide complex and its electronic feature is almost identical with that of $Cu(C_2H_4)$, Ag and acetylene *encountered within rare-gas matrices* form only a pseudocomplex.

The Ag–acetylene adduct formed in the vapor phase is clearly an example of the bonding scheme II. Since this scheme involves a rupture of a π bond, it is not surprising that an activation energy is required for its formation. We reported earlier that Al and acetylene cocondensed in a neon matrix also react to form an adduct having the vinyl structure.[19] A more recent study indicates that the formation of the Al–acetylene adduct also occurs in the vapor phase.[20] That Ag and ethylene do not interact in the vapor phase to yield the corresponding adduct must signify the difference in the energetics involved. The bond strength of the Ag–C σ bond is thus estimated to be larger than 58 kcal (the difference between the bond strengths of the carbon–carbon triple and double bonds), but less than 84 kcal (the difference between the carbon–carbon double and single bonds).

The experimentally determined A_{iso}'s of the vinyl radical,[13,21] the Al–acetylene,[19] and the Ag–acetylene adducts are compared below. The numbers in parentheses are the coupling

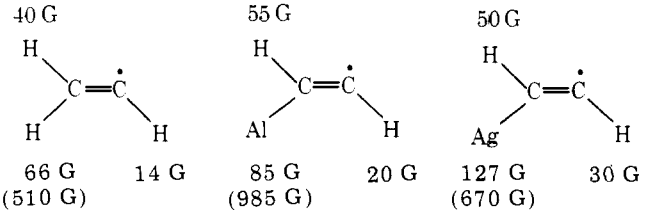

constants expected from a unit spin density in the H(1s), Al(3s), and Ag(5s) orbitals, respectively. The proximity of the spin density distributions in these radicals is conspicuous. It has been shown that the α-proton coupling constants of the vinyl radical and Al–acetylene adduct are positive and the $C{=}C_\alpha{-}H_\alpha$ sections of these radicals are bent.[13,19,21] The coupling constant determined for the α proton of Ag–acetylene is too large to be that of a proton located at the nodal plane of the p_π orbital of the terminal carbon. We believe that the α-proton coupling constant of Ag–acetylene is positive and its $C{=}C_\alpha{-}H_\alpha$ section is also bent. The α-proton coupling con-

stant thus increases in the order of the vinyl radical, Al-acetylene, and Ag-acetylene adduct, and indicates an increase in the angle of bend of the $C{=}C_\alpha{-}H_\alpha$ section in the same order.

The two most plausible structures for the Cu-diethylene and Cu-diacetylene complexes are (i) that in which the Cu atom is flanked by the two ligands oriented perpendicular to each other and (ii) that in which the Cu atom is flanked by the two ligands oriented parallel to each other. The two structures are of differing symmetry, D_{2d} and D_{2h}, respectively. In the D_{2d} arrangement (i), the d_{xz} and d_{yz} orbitals of Cu would interact

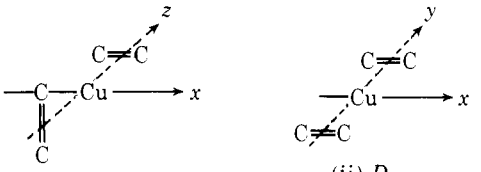

individually with the π^* orbitals of the respective ligands in a manner similar to that depicted in Figure 14 for the Cu-monoethylene case. The semifilled orbital of these complexes would then be correlated to Cu(4s), and a large, essentially isotropic hyperfine interaction with the Cu nucleus is predicted. The observed Cu coupling constants of both $Cu(C_2H_4)_2$ and $Cu(C_2H_2)_2$ are small and anisotropic. We suggest that these diligand complexes have the planar, D_{2h} structure (ii).

Figure 15 illustrates the interactions between the valence orbitals of Cu and the π and π^* orbitals of two ethylene molecules in the D_{2h} arrangement. It is immediately clear that the B_u orbital of the ligand section given by $\pi^*{-}\pi^{*\prime}$ interacts only with the $Cu(4p_x)$ orbital and would remain below the orbital correlated to Cu(4s). The semifilled orbital of the diligand complex is thus given by eq 10 and is illustrated below.

$$\Phi = a\phi_{Cu}(4p_x) + \frac{b}{\sqrt{2}}(\pi_y^* - \pi_y^{*\prime}) \qquad (10)$$

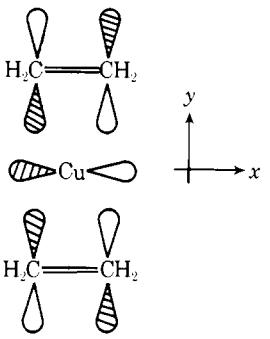

The actual wave function is probably dominated by the $Cu(4p_x)$ part ($a^2 > b^2$) reflecting the repulsive interaction imparted by the electrons in the bonding π orbitals. The analysis of the observed coupling tensors to the Cu nucleus in terms of eq 7 yields the following: for $Cu(C_2H_2)_2$,

$$A_{iso}(Cu) = -45.3\ G\ (-127\ MHz)$$

$$A_{dip}(Cu) = +22.7\ G\ (63\ MHz)$$

for $Cu(C_2H_4)_2$, equating $|A_\parallel| = A_1$ and $|A_\perp| = (A_2 + A_3)/2$,

$$A_{iso}(Cu) = -24.3\ G\ (-68\ MHz)$$

$$A_{dip}(Cu) = +27.2\ G\ (76\ MHz)$$

The negative A_{iso}'s determined above are of the magnitude expected from the polarization of the filled core orbitals. The magnitudes of A_{dip}'s determined above are very close to the

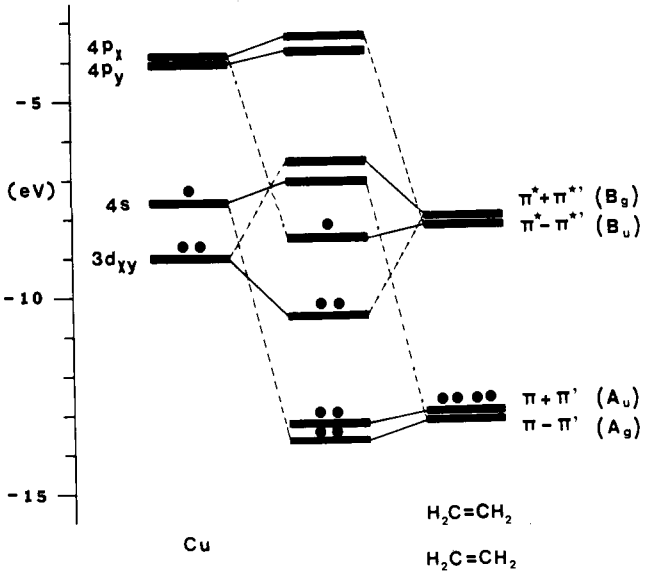

Figure 15. Schematic energy diagram showing the interaction between the valence orbitals of Cu and the π and π^* orbitals of two ethylene molecules in the D_{2h} arrangement.

A_{dip} of 68 MHz estimated earlier for a unit spin density in the Cu(4p) orbital. Though the latter value is clearly inadequate for accurate determination of the spin density distribution, the result obtained above strongly suggests that the semifilled orbital of these biligand complexes is essentially $Cu(4p_x)$.

The presence of large, isotropic interaction with the protons in the case of $Cu(C_2H_2)_2$, and the near total absence of the proton interaction in the case of $Cu(C_2H_4)_2$ are also in support of the proposed planar structure and the deduced semifilled orbital. In the former all the protons are located within the xy plane, and large, direct overlap occurs between the $Cu(4p_x)$ and each H(1s) orbital. In the latter case the protons are projected above and below the xy plane and the corresponding overlap is diminished.

The coupling interaction with the Ag nucleus in the case of $Ag(C_2H_4)_2$ is also small and anisotropic. It is suggested that $Ag(C_2H_4)_2$ also has the D_{2h} structure (ii) and the semifilled orbital similar to that given in eq 10 for $Cu(C_2H_4)_2$. We may then assert that the Ag coupling tensor be approximately axially symmetric about the x axis, and its magnitude be minimum in the x direction as in the cases of $Cu(C_2H_2)_2$ and $Cu(C_2H_4)_2$. We shall, therefore, set

$$|A_\parallel| = A_2 = 10.2\ G$$

$$|A_\perp| = (A_1 + A_3)/2 = 19.5\ G$$

The analysis of these quantities in terms of eq 7 yields

$$A_{iso}(Ag) = -9.6\ G \text{ and } A_{dip}(Ag) = +9.9\ G$$

or

$$A_{iso}(Ag) = -16.4\ G \text{ and } A_{dip}(Ag) = +3.1\ G$$

The small, negative, isotropic term is attributed to the polarization of the filled core orbitals, and A_{dip} to the occupation of $Ag(5p_x)$. The magnitude of A_{dip} for a unit spin density in the $Ag(5p_x)$ orbital was estimated to be 9 G from the fine structure spacing of the atomic spectrum of Ag at $^2P(4d^{10}5p^1)$ state.[18] The first set of A_{iso} and A_{dip} assessed above thus implies the dominance of $Ag(5p_x)$ in the semifilled orbital, while the second set places $\sim 1/3$ of the spin density in $Ag(5p_x)$ and the remaining in the B_u orbital of the diethylene group. The latter set is probably the correct one since it would account for the orthorhombicity of the Ag coupling tensor and the presence

of small but significant hyperfine interaction with the protons. However, this conclusion must be regarded as tentative in view of the assumption and approximation involved.

The deduced structures of the Cu and Ag complexes examined in the present study are shown schematically in Table II. Recently, Upton and Goddard reported on the result of an ab initio theoretical study (GVB-CI) of π-coordinated $Ni(C_2H_2)$ and $Ni(C_2H_4)$ with geometry optimization. They found very little distortion of the acetylene and ethylene ligands from the respective linear and planar structures, and very little delocalization of the orbitals. The Ni atom was found to be essentially $Ni(3d^94s^1)$ with the 4s orbital hybridized as 4s–4p pointing away from the ligand. The formation of the complexes is attributed to the attractive interaction between the π electrons and the partially unshielded Ni atom. The same mechanism must be operative in the formation of $Cu(C_2H_2)$ and $Cu(C_2H_4)$. The geometry of bis(ethylene)nickel has been examined by Rösch and Hoffman using the extended Hückel-type MO method.[23] They found that the two extreme structures of $Ni(C_2H_4)_2$, D_{2d} and D_{2h}, are essentially degenerate in the total energy ($\Delta E = 0.07$ eV) with no rotational barrier. Inspection of the energy diagram determined for $Ni(C_2H_4)_2$ as a function of the torsional angle (Figure 5 in ref 23) shows that the $Ni(C_2H_4)_2^-$ or $Cu(C_2H_4)$ would be more stable in the D_{2h} structure by ~0.8 eV.

References and Notes

(1) See, for example, a collection of review articles: *Angew. Chem., Int. Ed. Engl.*, **14**, 273 (1975).
(2) P. H. Kasai and D. McLeod, Jr., *J. Am. Chem. Soc.*, **97**, 6602 (1975).
(3) P. H. Kasai and D. McLeod, Jr., *J. Am. Chem. Soc.*, **100**, 625 (1978).
(4) H. Huber, D. McIntosh, and G. A. Ozin, *J. Organomet. Chem.*, **112**, C50 (1976).
(5) Cited in G. A. Ozin, *Acc. Chem. Res.*, **10**, 21 (1977).
(6) D. McIntosh and G. A. Ozin, *J. Organomet. Chem.*, **121**, 127 (1976).
(7) See, for example, L. J. Andrews and R. M. Keefer, "Molecular Complexes in Organic Chemistry", Holden-Day, Amsterdam, 1964.
(8) M. J. S. Dewar, *Bull. Soc. Chim. Fr.*, **18**, C79 (1951).
(9) J. Chatt and L. A. Duncanson, *J. Chem. Soc.*, 2939 (1953).
(10) P. H. Kasai, *Acc. Chem. Res.*, **4**, 329 (1971).
(11) P. H. Kasai and D. McLeod, Jr., *J. Chem. Phys.*, **55**, 1566 (1971).
(12) See, for example, M. W. Strandberg, "Microwave Spectroscopy", Methuen, London, 1954, p 11.
(13) P. H. Kasai, *J. Am. Chem. Soc.*, **94**, 5950 (1972).
(14) B. Bleaney, *Philos. Mag.*, **42**, 441 (1951).
(15) E. Rytter and D. M. Gruen, *Spectrochim. Acta, Part A*, **35**, 199 (1979).
(16) H. M. McConnel and J. Strathdee, *Mol. Phys.*, **2**, 129 (1959).
(17) For the analysis of hyperfine coupling tensors, see, for example, P. W. Atkins and M. C. R. Symons, "The Structure of Inorganic Radicals", Elsevier, Amsterdam, 1967.
(18) C. E. Moore, *Natl. Bur. Stand. (U.S.), Circ.*, **No. 467**, 1 (1949); 2 (1952); 3 (1958).
(19) P. H. Kasai, D. McLeod, Jr., and T. Watanabe, *J. Am. Chem. Soc.*, **99**, 3521 (1977).
(20) P. H. Kasai and D. McLeod, Jr., unpublished result.
(21) E. L. Cochran, F. J. Adrian, and V. A. Bowers, *J. Chem. Phys.*, **40**, 213 (1964).
(22) T. H. Upton and W. A. Goddard, III, *J. Am. Chem. Soc.*, **100**, 321 (1978).
(23) N. Rösch and R. Hoffmann, *Inorg. Chem.*, **13**, 2656 (1974).

A Convenient Synthesis of Cyclopentanones via Rhodium(I)-Catalyzed Intramolecular Hydroacylation of Unsaturated Aldehydes

R. C. Larock,*[1] K. Oertle, and G. F. Potter

Contribution from the Department of Chemistry, Iowa State University, Ames, Iowa 50011.

Received May 14, 1979

Abstract: The rhodium(I)-catalyzed intramolecular hydroacylation of unsaturated aldehydes has been investigated. Three useful new catalyst systems have been developed. The catalysts are prepared by the addition of 2 equiv of tri-*p*-tolylphosphine, tri-*p*-anisylphosphine, or tris(*p*-dimethylaminophenyl)phosphine to chlorobis(cyclooctene)rhodium(I) in ethylene-saturated methylene chloride. 4,5-Unsaturated aldehydes afford good yields of substituted cyclopentanones. However, alkyl substitution in either the 2 or the 5 position substantially reduces the yield of ketone. Disubstitution in the 2 position gives rise to ethyl ketones instead. This procedure provides a valuable new route to spirocyclic and fused bicyclic ketones, but is not applicable to the synthesis of ketones of ring size other than five. Furthermore, it is tolerant of almost all important organic functionality except amines.

The transition metal catalyzed hydroformylation or oxo reaction is an extremely important industrial process which has been the subject of numerous studies (eq 1).[2-5] On the

$$RCH{=}CH_2 + CO + H_2 \longrightarrow RCH_2CH_2\overset{\overset{O}{\|}}{C}H \qquad (1)$$

other hand, relatively few methods exist for the addition of aldehydes to olefins and each has severe limitations (eq 2).[6-12]

$$RCH{=}CH_2 + \overset{\overset{O}{\|}}{H}CR' \longrightarrow RCH_2CH_2\overset{\overset{O}{\|}}{C}R' \qquad (2)$$

In this study we wish to report the development of several useful new catalysts for the intramolecular cyclization of 4,5-unsaturated aldehydes to cyclopentanones. Although numerous examples of the cationic cyclization of 5,6- and 6,7-unsaturated aldehydes to six- and seven-membered rings are known,[13-27] similar attempts to generate five-membered rings have generally failed.[27] However, Sakai and co-workers have reported that 2- and 3-substituted 4-pentenals could be cyclized to the corresponding cyclopentanones using *equivalent* amounts of either stannic chloride or Wilkinson's catalyst, $RhCl(PPh_3)_3$ (I) (eq 3).[28] Unfortunately, the yields were quite

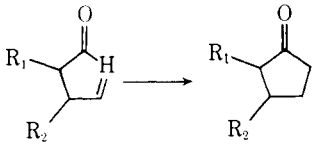

(3)

low (0–57 and 17–34%, respectively) and the tin reaction, although highly stereospecific,[29] requires substitution α to the carbonyl. Lochow and Miller subsequently observed that 4-pentenal can be *catalytically* cyclized to cyclopentanone

0002-7863/80/1502-0190$01.00/0